Limits on Pluto's Ring System from the Jun 12 2006 Stellar Occultation and Implications for the New Horizons Impact Hazard

Henry B. Throop

Planetary Science Institute

1700 E Fort Lowell Rd #106

Tucson, AZ 85719

and

Physics Department, University of Pretoria

Hatfield, Pretoria, South Africa

throop@psi.edu

Richard G. French

Wellesley College

Wellesley, MA 02481

Kevin Shoemaker

Shoemaker Labs

2225 Hwy A1A, #311

Indian Harbour Beach, FL 32937

Cathy B. Olkin, Trina R. Ruhland (*), Leslie A. Young

Southwest Research Institute

Boulder, CO 80302

* Current affiliation: Miner's View Observatory, Breckenridge, CO 80424

Submitted to *Icarus* 20-Dec-2013; Revised 1-May-2014; Accepted 14-May-2014

Received _____; accepted _____

Abstract

The Pluto system passed in front of a 15th magnitude star on 12 Jun 2006. We observed this occultation from the 3.9 m Anglo-Australian Telescope (AAT), and took photometric observations every 100 msec for three hours. Our three-hour baseline of data provides among the longest and highest-quality occultation dataset of the Pluto system ever taken. Results on Pluto's atmospheric structure from these data have been previously reported (Young *et al.* 2008). Here we report on limits for rings, ring arcs, and small satellites within the system. We find a 3σ upper limit on the normal optical depth of $\tau < 0.07$ for narrow rings of width 2.4 km, and $\tau < 5 \times 10^{-3}$ for rings of width 1500 km. We also detect no discrete objects of radius 220 m or larger along the occultation path. Motivated by the upcoming flyby of New Horizons through the Pluto system, we estimate the dust impact hazard to the spacecraft based on our optical depth limits and those derived from imaging with the Hubble Space Telescope.

1. Introduction and Motivation

Stellar occultations have been used to study and detect planetary rings throughout the solar system, from Saturn to Uranus to Neptune (Guinan *et al.* 1982; Colwell *et al.* 2010; Elliot *et al.* 1977). Rings have been hypothesized at Pluto, but never detected (Stern *et al.* 2006; Durda and Stern 2000). In the Pluto system, rings might be created when interplanetary dust particles impact the smaller satellites (Nix, Hydra, Kerberos, and Styx), where the ejecta velocity can exceed the local escape velocity. Once formed, rings from this dust could be self-sustaining, as ring particles re-impact the satellites and excavate new material, or unseen ring-moons within the ring collide and release debris. In the former

case the rings would be near the orbits of the known satellites, while in the latter case they need not be. Although all of Pluto's known satellites lie within 1° of the same plane, the system's displaced barycenter may cause rings to have different characteristics than in the other planetary systems. For instance, at Jupiter and Saturn, rings are stable at several planetary radii from the central body. But at Pluto, this region is dynamically unstable (Giuliatti Winter *et al.* 2013; Pires dos Santos *et al.* 2013).

Our interest in the ring system has a secondary motivation: the New Horizons spacecraft is set to fly past Pluto in July 2015. While passing by Pluto, New Horizons will perform searches for rings and debris and will substantially improve on Earth-based measurements, due to both its proximity and its ability to observe at the high phase angles where small dust grains appear much brighter. Constraints on the ring system determined in advance of the encounter will help plan science observations, and help identify any particularly safe or unsafe paths through the system.

1.1. Stellar occultations of rings

Although direct imaging is the most common method of studying rings, occultations have some distinct advantages. The ring systems of both Uranus and Neptune were detected by stellar occultations before they were imaged (Guinan *et al.* 1982; Elliot *et al.* 1977), and occultations were recently used to detect a ring system surrounding the asteroid Chariklo (Braga-Ribas *et al.* 2014). In the Saturn system, ring occultations are frequently observed with Cassini to study structure at scales much smaller than the imaging resolution limit.

The theoretical resolution limit for occultation observations is given by the Fresnel diffraction limit, which specifies the spatial resolution δR in terms of the distance D and

wavelength λ,

$$\delta R = (D\,\lambda/2)^{1/2}. \quad (1)$$

In the case of Cassini observing Saturn's rings in the UV from a typical distance $D = 80,000$ km (Colwell *et al.* 2010), the Fresnel limit is roughly 2 m, better by 50× than the best-possible imaging resolution from the same sized aperture at the same distance. For the Pluto occultation studied here, the Fresnel scale in the optical is 2 km, while the Hubble Space Telescope's resolution limit at Pluto's distance is roughly 1500 km.

Stellar occultations offer a second advantage: because the total flux is spatially summed, observations are relatively insensitive to stray light or PSF issues. This allows for measurements to continue with little loss in sensitivity even as the occulting body approaches the star. Direct imaging is often limited by stray light, in particular when searching for faint features such as rings at sub-arcsecond separations from a bright planet.

Since 1988, Pluto has been probed by more than 15 stellar occultations, yielding more than 90 light curves. While most of these observations have been used to study Pluto's atmosphere, some of the existing data can also be used to search for serendipitous occultations of rings or debris.

Stern *et al.* (2006) predicted rings near Nix and Hydra of optical depth $\tau \approx 5 \times 10^{-6}$. Searches for rings here or elsewhere in the system have so far detected nothing (Boissel *et al.* 2014; McKay 2008; Steffl and Stern 2007; Pasachoff *et al.* 2006). In this paper, we present results which improve the upper limit on the putative Plutonian rings.

2. Experimental Details

2.1. Observations and Data Reduction

We study here the occultation of a 15th magnitude star on 2006 Jun 12, visible from the Earth's southern hemisphere. Two groups observed this occultation in order to study Pluto's atmosphere (Young *et al.* 2008; Elliot *et al.* 2007). This occultation is particularly useful for searching for rings for several reasons. First, the occultation star is reasonably bright. Second, the shadow passed directly over the 3.9-m Anglo-Australian Telescope (AAT) at Sliding Springs, Australia on a clear night. And third, at the AAT we acquired a particularly long dataset, covering the star's apparent path behind not just Pluto, but the entire Pluto system. These three factors make this dataset particularly valuable to search for unknown objects in the Pluto system.

RF and KS used the $f/8$ AAT to observe the occultation of the star P384.2 (McDonald and Elliot 2000), *i.e.*, UCAC2 2603 9859 (M_V=15.0, with 2MASS magnitudes M_J=12.299 and M_K=11.311). The sky was extremely clear, following very stormy weather in the days before the event. The moon was nearly full and $\sim 10^\circ$ from Pluto. Images were taken using a Princeton Instruments MicroMax BFT512 CCD at 10 Hz, binned on-chip from 256×256 to 64×64 pixels (Young *et al.* 2011). This detector has both low noise (3 e^- per read) and a very short dead time between exposures (2 msec, yielding 98 msec integrations). The binned resolution was 0.348 arcsec per pixel. The occultation center was at approximately t_0 = 2006 Jun 12 16:23:21 UT. We observed from roughly $t_0 - 122$ min to $t_0 + 33$ min. Data were taken continually, except for $\sim$ 1-minute gaps every 20 minutes in order to download data and synchronize clocks. 86,800 individual frames were taken. The time for the path of Pluto's outermost satellite Hydra to pass entirely across P384.2 was approximately one hour, so the occultation covered the region inside and outside of the satellite orbits. The shadow velocity v_s was 23.6 km/sec, giving us a per-sample resolution of 2.36 km,

approaching the Fresnel limit of 2 km. A typical frame is shown in Fig 1, and a plot of the occultation path in the sky plane is in Fig. 2.

Our data reduction was done with a heavily modified version of the pipeline discussed in Young *et al.* (2008). First, all frames were calibrated and dark-subtracted. The positions of Pluto, P384.2, and two comparison stars were determined on each frame individually using a centroid method (M. Buie's IDL `CENTROD` routine[1], Buie 1996). We initially did the photometric analysis using a PSF-fitting routine (the IDL astrolib `CNTRD` function, based on DAOPHOT), but found it difficult to obtain consistent photometric results. We switched to aperture photometry (M. Buie's IDL routine `BASPHOTE`) and were able to consistently measure the brightness of all four objects, which were of roughly comparable flux. When the objects were clearly separated from each other, we used the smallest aperture possible to minimize noise; this was usually 3.1–3.5 pixels. However, because Pluto moved ~ 15 pixels during the observation, we changed our aperture size as needed. At separations of up to 7.5 pixels we used one large aperture containing both Pluto and P384.2, while at greater separations we used two smaller apertures. We determined the distance limit of 7.5 pixels by testing our pipeline over a range of separations and aperture sizes.

After our raw light curve was produced, we removed frame-to-frame variations by dividing by the mean flux of the two comparison stars. We also fit and subtracted a low-order polynomial in order to remove systematic trends due to atmospheric or instrumental changes. This high-pass filtering reduces our sensitivity to faint rings on scales >10,000 km, for which imaging is intrinsically much more sensitive than occultations. The curve was then normalized by setting the flux at the occultation to zero. We found the maximum SNR per scale-height (60 km) in the range 200-350 (Fig. 5), in line with Young *et al.* (2008). Our SNR changes during the event because the aperture size is adjusted

[1] `http://www.boulder.swri.edu/~buie/idl`

to account for Pluto's motion, with SNR reaching its maximum when the aperture is the smallest.

2.2. Measurement of optical depth

The light curve can be used to measure the properties of the rings or bodies passing in front of the star. In the case of a broad ring (of width exceeding the Fresnel radius) passing in front of a distant star, the observed stellar flux drops from I_0 to I. The ring's optical depth τ can then be determined by measuring the fluxes and applying

$$I = I_0\, e^{-\tau/\mu}\ . \tag{2}$$

The cosine of the ring tilt angle is given by μ; for a ring seen fully-open $\mu = 1$, while for this event $\mu = \cos(36.6^\circ)$. The normal optical depth τ_n is given by

$$\tau_n(\lambda) = \int n(r)\, \pi r^2\, Q_{ext}(r, \lambda)\ dr, \tag{3}$$

where Q_{ext} is the extinction efficiency at wavelength λ. The radius of an individual scatterer is r, and the size distribution is defined by $n(r)$. In the limit $r \gg \lambda$, Q_{ext} reaches the limit 2 (not 1), because light is both scattered *and* diffracted out of the beam. The particle albedo does not enter into Eq. 3.

An occultation can also occur not from a ring, but from a discrete body. Consider the case of a round body passing in front of the star, where the body has an angular size much larger than the star's and is able to fully extinguish the star's light for some time Δt. Ignoring diffraction effects, the size can be calculated from

$$I = I_0(1 - \frac{l}{v_s \Delta t}) \tag{4}$$

where l is the chord length across the occulter and v_s is the apparent shadow velocity across the star. For a circular body, the average chord length is $l = \sqrt{2}r$, where r is the body's radius. Eq. 4 applies where the angular size of the star is less than that of the occulter. For the case of P384.2, we used the star's magnitude and color to calculate a projected stellar radius of 320 m at 30 AU (van Belle 1999), so this condition in Eq. 4 holds. Diffraction effects cause the light curve by a small occulter to be more complex than a simple 'top hat' profile (Boissel *et al.* 2014). Because we are sampling the data at roughly the Fresnel resolution, and the occultation depth is small, most of this structure in the wings is not visible and the occultation is essentially a dip one or two bins wide.

3. Results

3.1. Limits from full-resolution data

Our reduced light curve is shown in Figs. 3–4. The first figure shows the entire 2.5-hour event, while the latter presents just the central hour where the star crossed the orbits of all five satellites. In neither plot are there any features which are immediately obvious as indicating rings or debris. Although a few individual points are noticeable, there are no obvious cases in either dataset where multiple consecutive measurements are all outside the norm.

We can search for statistically significant outliers. The standard deviation of the normalized intensity for the central hour (excluding the occultation) is $\sigma = 0.027$. Assuming Poisson statistics of these $N \approx 34,000$ points, we would expect 1.2 individual points to exceed 4σ from the mean, and we found two such points. At 5σ from the mean, we expect to find 0.01 points, and found zero. Thus, we do not detect any substantial outliers at any standard deviation level. Our 3σ detection limit is therefore an occultation depth

$1 - I/I_0 = 0.08$. This corresponds to a limit of $\tau_n < 0.069$ for rings of width 2.4 km (Eq. 2).

For individual bodies, the 5σ upper limit implies a maximum occulter chord length of $l < 320\,\mathrm{m}$, or a radius of $r < 220\,\mathrm{m}$. Any discrete bodies larger than this in the path would have been detected in the data. We recorded zero points at 5σ from the mean, so our observation puts a firm upper limit on this population along the path.

3.2. Limits from binned data

The limits above come from the full resolution data. However, resampling the data to lower resolution allows us to both increase the sensitivity and compare to previous searches. For instance, Steffl and Stern (2007) searched at a radial resolution of 1500 km, dictated by HST's spatial resolution. In order to compare, we have binned our data to 1500 km, 100 km, and 5 km. For all these cases, we resampled the raw data by convolving with a triangular kernel of halfwidth equal to the specified resolution. We found the triangular kernel to produce smoother and more useful results than ether a boxcar smoothing or a sinc-based algorithm (Buie's `SINCFLTR` routine).

Fig. 4 presents both the raw and resampled data. In the same way as we measured the limit for the unbinned data, we have measured the maximum 3σ occultation depths (that is, $1 - I/I_0$), which can be then used to calculate the optical depth limit. These values are presented in Table 1.

Examining the smoothed data by eye, there are again no clear dips that stand out. The largest and most consistent feature is a 50-second ($\sim$ 1200 km) blip centered at 600 sec, near Charon's orbit. The feature is visible in all three smoothed curves and has magnitude $\sim 1\%$. However, it is a signal increase, not a drop, so it is clearly not an occultation. If it were a dip, such a large object would have been detected long ago by imaging. The blip disappears

when using either a smaller or larger aperture, so it may be a seeing-related transient; its magnitude is consistent with our 1σ error levels. A second feature shows a roughly 1% decreasing trend in flux in the few minutes after the end of the Pluto occultation, perhaps mirrored by a rising trend just before the occultation. Although such a signal looks tantalizingly like that which might be produced by a faint dust atmosphere surrounding Pluto, detailed examination of the raw photometry at multiple apertures shows that this is almost certainly due to Pluto's PSF wings moving very slightly out of its 3.5-pixel radius aperture. We have found no features larger than these two, as either drops or increases.

3.3. Satellite positions

Because rings are often found in close proximity to satellites, we wanted to search for correlations in our data between the orbits of the known satellites and any possible features. To do this, we used the JPL SPICE libraries[2] to compute the positions of Pluto's four satellites at the predicted occultation center time. The positions were calculated using the JPL-provided kernel files `plu017.bsp` (Pluto, Charon, Nix, Hydra), `plu020.bsp` (Kerberos, C. Acton 2011), and `p4p5.revised.bsp` (Styx, R. Jacobsen 2013). We then computed their orbital paths by calculating the positions that each body would take when moved through an entire circular orbit about Pluto's barycenter. Real rings could have more complex orbits, but for this search, a more complex model is not justified. We applied a timing offset of -90 sec to the computed times, accounting for errors in the pre-occultation knowledge of the star's position (Assafin *et al.* 2010). Our resulting orbit crossing times are plotted against the data in Fig. 4. Also plotted is the position of closest approach between the star and Nix, at a projected distance of ~ 1500 km. All other possible satellite occultations were

[2]`http://naif.jpl.nasa.gov/naif`

at much further distances and are not plotted.

Looking at Fig. 4, there are no features in any of the curves which appear to correlate with the orbital crossings, even at low confidence levels, nor is there any obvious feature associated with the near-occultation of Nix.

4. Comparison with other occultations

Several previous reports have also searched for Pluto's rings using occultation data. McKay (2008) and Pasachoff *et al.* (2006) report on a different dataset taken in Australia during the same 2006 occultation that we study here. They did not detect the ring, but placed a limit of $\tau \lesssim$ 0.2–0.04, depending on the binning width used. Boissel *et al.* (2014) used five light curves from two events (April 10 2006 appulse and June 14 2007 occultation) to measure the ring abundance. None of the events detected any material; the tightest constraint was from the slow 6 km/sec 2006 event as seen by the 8.2 m Very Large Telescope (VLT) in Chile. From this event, they calculated the 'equivalent width' in transmission to be $EW \approx W\,\tau_n < 30 - 100\,\mathrm{m}$, for rings of width W less than 10 km. Converting this to τ_n, their limits are a few times better than ours, consistent with the larger aperture and slower shadow velocity of their event. The VLT curve sampled the region from roughly Charon to Hydra on one side of Pluto only; our light curve goes to the surface of Pluto, and extends to Hydra on both sides.

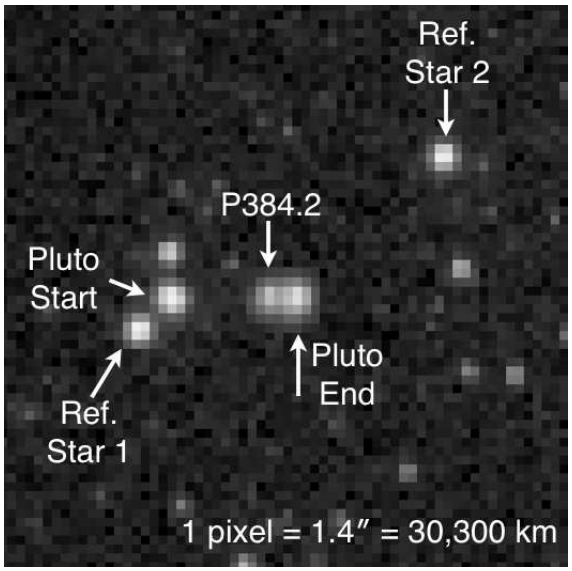

Fig. 1.— Sample image from the start of the observation. A sub-image of Pluto at its final position has been superimposed. Pluto moves from left to right in this image, which is 64 × 64 pixels.

Search and binning	3σ **Upper Limit**
Rings, 2.4 km (no binning)	$\tau_n < 6.9 \times 10^{-2}$
Rings, 5 km	$\tau_n < 2.6 \times 10^{-2}$
Rings, 100 km	$\tau_n < 8.5 \times 10^{-3}$
Rings, 1500 km	$\tau_n < 4.7 \times 10^{-3}$
Satellites along occultation path	$r < 220\,\mathrm{m}$ (5σ)

Table 1: Results of search for rings in 2006 Jun 12 AAT stellar occultation. These limits apply in the central region near Pluto and Charon; limits are ~2× higher at the orbit of Hydra.

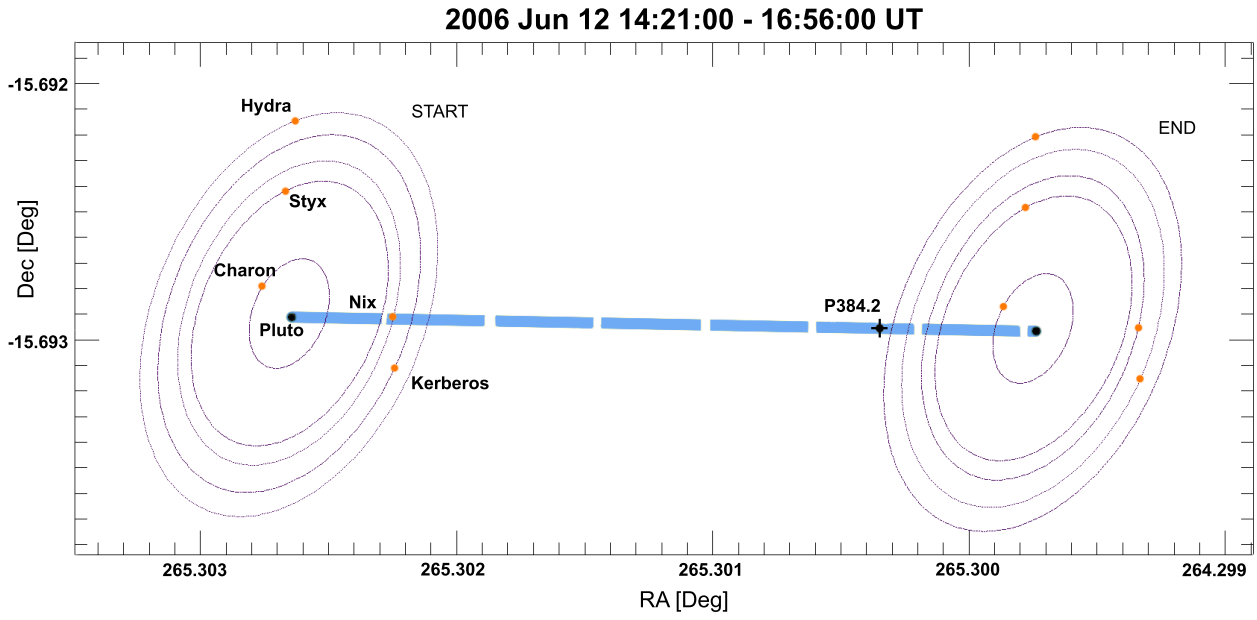

Fig. 2.— Diagram of occultation geometry. Pluto moves from left to right on this image. Orbital direction of the satellites is counterclockwise. The blue bar shows Pluto's path, with the gaps indicating where observations were not taken due to data readout. Created with GeoViz, `http://soc.boulder.swri.edu/nhgv` (Throop *et al.* 2009).

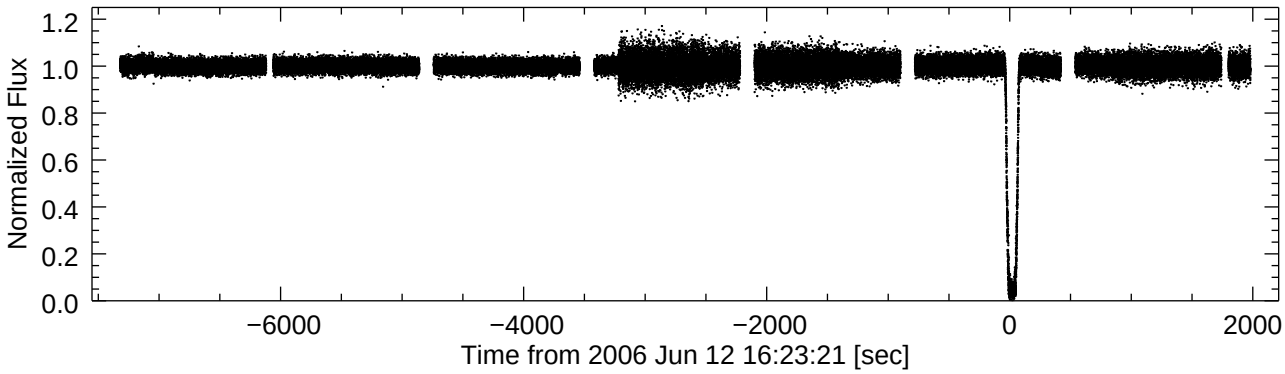

Fig. 3.— Reduced light curve, full 2.5 hour dataset. The initial portion (to $t = -3200$ sec) is the brightness of star P384.2 alone, measured using a photometric aperture of radius 3.5 pixels. In later frames, Pluto has moved close enough to the stars so that they can no longer be measured in separate apertures, so we switch to a larger 7.5-pixel aperture in our reduction pipeline in order to accommodate both objects. The aperture radius is then slowly decreased to 3.5 pixels at the occultation center, and increased afterwards. The larger apertures result in lower SNR. The curve is normalized such that a level of zero indicates that the star is fully occulted. These data have been calibrated against our standard stars to remove frame-by-frame variations, and individual segments have been flattened using a low-order polynomial. The gaps every ~ 20 minutes are where observations were paused for data download and clock synchronization.

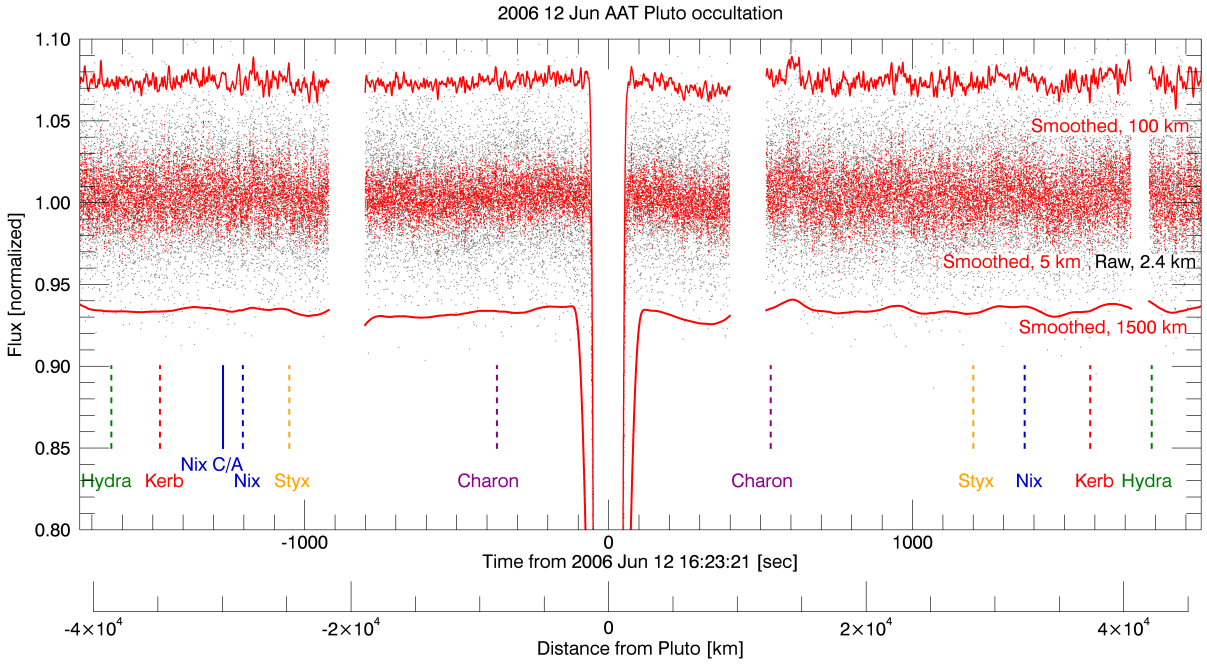

Fig. 4.— Light curve for central hour surrounding occultation. Full-resolution data (black) are plotted along with smoothed data (red), to which an arbitrary vertical offset has been applied. The locations of the satellite orbits crossings are marked, as is the location of a 1500 km near-occultation by Nix.

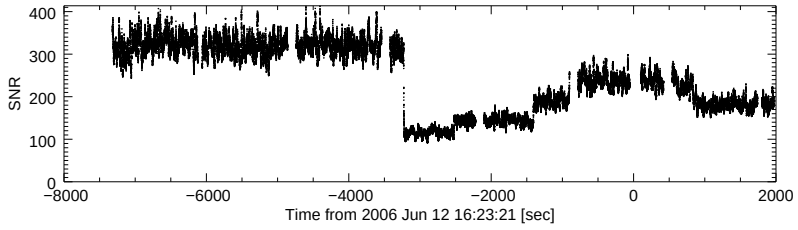

Fig. 5.— Signal-to-noise ratio of P384.2 during the observation. The change in SNR is due to the variable-sized aperture used in analysis.

5. Comparison with direct imaging

Direct imaging can also been used to search for Pluto's rings. I/F is usually used to measure reflected ring brightness, and is defined as

$$\frac{I}{F} = \frac{\tau a}{\mu} \tag{5}$$

where the optical depth in reflected light is

$$\tau(\lambda) = \int n(r)\, \pi r^2\, Q_{sca}(r, \lambda)\, dr. \tag{6}$$

a is the particle albedo, and unlike the occultation case (Eq. 3), the detection threshold does depend on a.

Steffl and Stern (2007) used the Hubble Space Telescope (HST) to measure the I/F directly from images. The limiting factor in their observations was stray light from Pluto and Charon, which could not be easily removed. Assuming an albedo $a = 0.04$, they concluded that $\tau \lesssim 10^{-5}$ at the orbit of Nix, with higher limits increasing inward (Fig. 6).

Two additional HST programs also searched for the rings, in June 2011[3] and June-July 2012[4]. These observations rolled the telescope strategically so as to optimize the subtraction of stray light from Pluto and Charon. Preliminary results from these programs (Showalter *et al.* 2012; M. Showalter personal communication) find $\tau < 3 \times 10^{-7}$ for the Charon region and $\tau < 10^{-7}$ for the region of the outer four satellites. It is unlikely that any future HST observations can improve significantly on these because of the intrinsic limits to stray light rejection.

---

[3]DD-12346, 5 orbits, PI Showalter

[4]DD-12801, 34 orbits, PI Weaver

The HST limit is 4-5 orders of magnitude better than the AAT occultation data, depending on the orbital distance and albedo assumed. The AAT data probe closer to Pluto's surface than can the HST observations, but beyond 5,000 km from Pluto, the HST limit is superior.

6. Implications for New Horizons

The New Horizons (NH) spacecraft will pass near the Pluto system during its July 14 2015 encounter. Its nominal trajectory will take it through the system's equatorial plane at a distance of some 10,000 km, roughly midway between Pluto and Charon. The trajectory was chosen to maximize scientific return, but other trajectories could be used if there was evidence to show that the region near Pluto is unsafe due to impact risk with potentially damaging dust grains. The NH mission defined a critical impact as one of radius $r_c = 200$ μm ($\sim 10^{-4}$ g) at NH's encounter velocity, and set the requirement that the spacecraft encounter $N < 0.1$ such impacts during the straight-line pass through the Pluto system. We have then

$$N = n(r > r_c) \frac{A}{\mu_{sc}} \tag{7}$$

where $A \approx 5.5$ m^2 is the cross-sectional area of the spacecraft, and μ_{sc} is the cosine of the sub-spacecraft latitude B_{sc} at closest approach. A trajectory directly through the plane will encounter fewer particles than one on a shallow slant angle; for the nominal NH encounter geometry, $\mu_{sc} \approx \cos(49°)$. Combining Eqs. 5–7, N can then be calculated exactly from τ or I/F, and the size distribution $n(r)$.

It is nearly impossible to directly measure the abundance of grains of size $r_c = 200\,\mu$m, because such grains are indistinguishable in the optical and IR from much larger and smaller

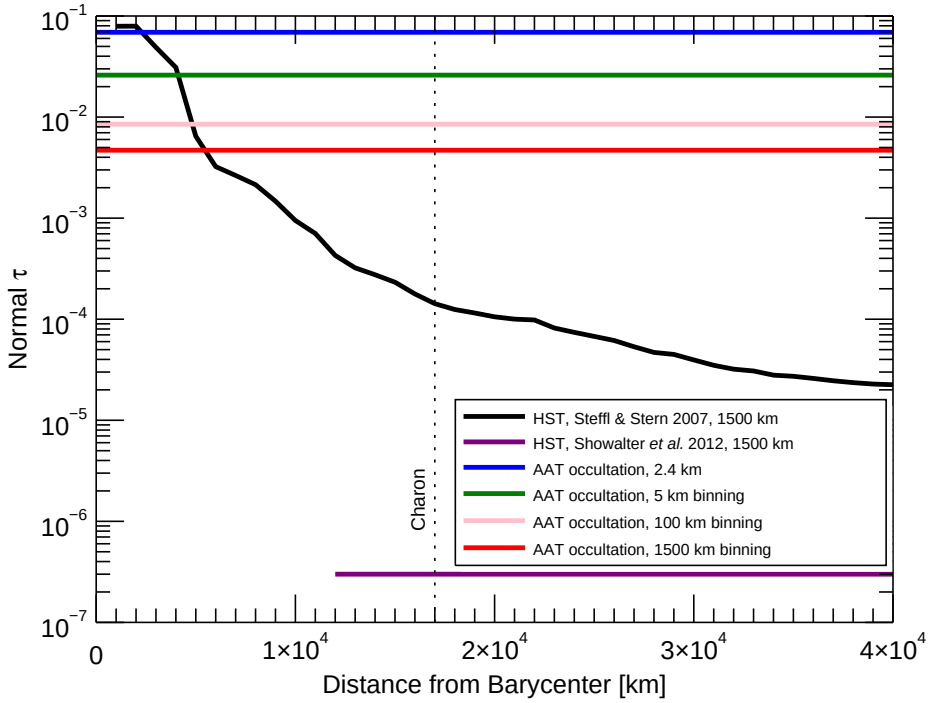

Fig. 6.— Observational upper limits for rings in the Pluto system. The 2007 HST observations are affected by stray light which increases toward to Pluto. The 2012 HST observations reduced stray light significantly but were saturated inward of 12,000 km. HST's spatial resolution was 1500 km. The occultation data are unaffected by stray light, and provide the best limit near the system barycenter. 2007 HST data provided by A. Steffl and adapted from Steffl and Stern (2007), and assumes albedo 0.04.

particles. Also, given a typical size distribution in rings, grains of this size are expected to be quite rare in proportion to the easily seen micron-sized grains. Therefore, rather than measure $n(r_c)$ directly, it must be inferred from observations at other wavelengths and from assumptions about the ring's intrinsic size distribution. An 'absolute worst case' scenario can be examined if we assume that 100% of the rings' optical depth is due to grains of radius exactly r_c. In this case, Eqs. 5 – 7 give us

$$N = \frac{I}{F} \frac{A}{\mu_{sc}\, a\, \pi r^2 Q_{sca}} \tag{8}$$

Plugging in the 2012 HST I/F limit and assuming an albedo $a = 0.05$, we find $N \approx 500$ – *i.e.*, loss of the mission. Thus the observations alone, when interpreted most conservatively, cannot technically rule out a danger to the spacecraft. However, in this case our input assumptions are truly extreme enough that the computed value of N does not make a useful statement about the actual danger.

In order to make a 'plausible worst case' scenario, we make the more reasonable assumption that the grains are distributed not unimodally but in a power law, where

$$n(r)\, dr = r^{-q}\, dr \ . \tag{9}$$

The exponent q indicates the slope of the distribution. Values of $q < 3$ indicate rings with most of their surface area in small grains, while $q > 3$ shows a dominance of large grains. Power laws are thought to be common in collisional systems such as rings. Even if the actual distribution is not a power law, by choosing a wide range of values if q, we are likely to bound the actual distribution.

Given the size distribution, the brightness of a ring can be predicted by applying a light scattering model. Mie scattering is typically used in the rings literature for the smallest grains. However, Mie becomes inaccurate for larger grains, because it assumes them to be

perfectly spherical, homogeneous, and smooth. Any cracks, voids, or surface roughness causes a grain to be more back-scattering (e.g., consider a hailstone vs. a water drop of the same size and composition). The size at which this transition from Mie to macroscopic (Lambertian) scattering occurs varies based on a particle's history and processing. Some experimental work has shown it to be in the 10–100 μm range (Schmitt et al., 1987), and a transition near this size was used to fit data from Saturn's G ring (Throop and Esposito 1998). In the current model, we choose a transition size of 300 μm, in order to be conservative and to acknowledge the possibility that Pluto's ring particles could conceivably be young, unprocessed grains from Triton-plumes on Pluto. For grains below this size we used Mie scattering to calculate Q explicitly; grains larger than this were taken to be Lambertian. The composition was assumed to be be a silicate-ice mixture with index of refraction $1.33 + 0.001i$ and albedo 0.05. The size range extended from $r = 0.01$ μm to $r = 5$ mm across 500 logarithmically spaced bins. We normalized n such that I/F (Eq. 5) matched that from HST. It was then straightforward to calculate N from Eq. 7. We calculated N for nine different size distributions, all power laws with q in the range 1.5–7. In order to validate our two-component light scattering model, we ran several test cases using the end-member cases, that is, the Mie scattering and Lambertian scattering alone. As expected, the model containing a mixture of these two scatterers was always bounded by the two single-component models (Fig. 7).

Results are shown in Fig. 8. The plot shows that for steep size distributions where $q \gtrsim 4$, New Horizons is out of the 'Danger' zone, receiving $N < 0.1$ dangerous hits. However, for $q \lesssim 3.5$, the spacecraft's safety cannot be assured by the observations alone. Values of q in the range 2–3 yield $N \lesssim 20$ dangerous hits through the encounter. Smaller values of q result in larger N, because these distributions are dominated by larger grains. Neither the size limits nor the composition strongly affect the results.

The actual size distribution at Pluto is of course unknown, but typical collisional ejecta has a $q_{ej} \approx 3.5$ upon initial creation (Durda *et al.* 2007). Size-dependent processes in planetary rings almost always reduce q: Poynting-Robertson drag and radiation pressure are both proportional to size, reducing q by 1. Recent numerical simulations of dust loss processes at Pluto support $q = q_{ej} - 1$ (Doug Hamilton, personal communication), suggesting that $q = 2.5$ would be reasonable for dust at Pluto. Because the curves for q =2–3 are similar near near r_c, the inferred value for N turns out to be only weakly sensitive to changes to q.

The albedo assumed is a conservative value, consistent with the low visual albedo of Uranus ring particles (Cuzzi 1985). Icy particles with a higher albedo are also prevalent in the outer solar system, but lacking any other constraints, we use the most conservative 'worst case' value available. The albedo of Pluto and Charon are in the range 0.3–0.5, suggesting the system's ring particles could have a high albedo; such bright particles would cause N to decrease.

It is clear that Fig. 8 does not by itself rule out a danger to the spacecraft if the size distribution is in the low-q range. As a result, the NH mission and independent groups have undertaken substantial dynamical modeling of the dust environment in the inner Pluto-Charon region. These studies have shown that the population of grains of r_c in the equatorial plane near NH's nominal trajectory is further reduced by a factor of ~ 100 due to dynamical clearing within the five-body system, making it unlikely to retain debris (Pires dos Santos *et al.* 2013; Giuliatti Winter *et al.* 2013). This places additional independent limits on the dust population. Using these constraints and a higher-fidelity model for spacecraft impact sensitivity, the NH project has independently calculated the upper limit to the probability of a loss-of-mission impact at 3×10^{-3} with a 95% confidence (Clayton Smith and S. Alan Stern, personal communications). In addition, the NH mission

has the option of diverting its encounter trajectory from the inner region of the system to a more distant flyby if imaging in the weeks before encounter indicates the presence of an unsafe dust population.

6.1. Future observations

Future occultations have the ability to improve the detection threshold for narrow rings around Pluto. In particular, appulses ('near-occultations') by bright stars which pass through the Pluto system are much more frequent than occultations of Pluto itself. These types of events have not usually been targeted in the past, but have substantial value in constraining the system's small body population.

For searches of satellites and broad rings, the limits placed by HST's direct imaging are unlikely to be challenged by other Earth-based observations in the foreseeable future.

The τ limit from the occultation could be improved with additional observations using brighter stars and/or larger telescopes. For instance, observing an occultation of an 11th magnitude star from a 10-m telescope would yield a signal 250× brighter the dataset used here, and an SNR some 15× better. However, such an increase in sensitivity would still be 100× higher than the limit from HST in the region of Nix and Hydra. Occultations will always be superior to HST for searching for small ring arcs and small objects near the Fresnel scale, and in the closest region toward the planet.

7. Acknowledgments

Thanks to Mark Showalter, Matthew Hedman, Hal Weaver, Alan Stern, and Doug Hamilton for comments. We also thank Mark Showalter and Andrew Steffl for providing

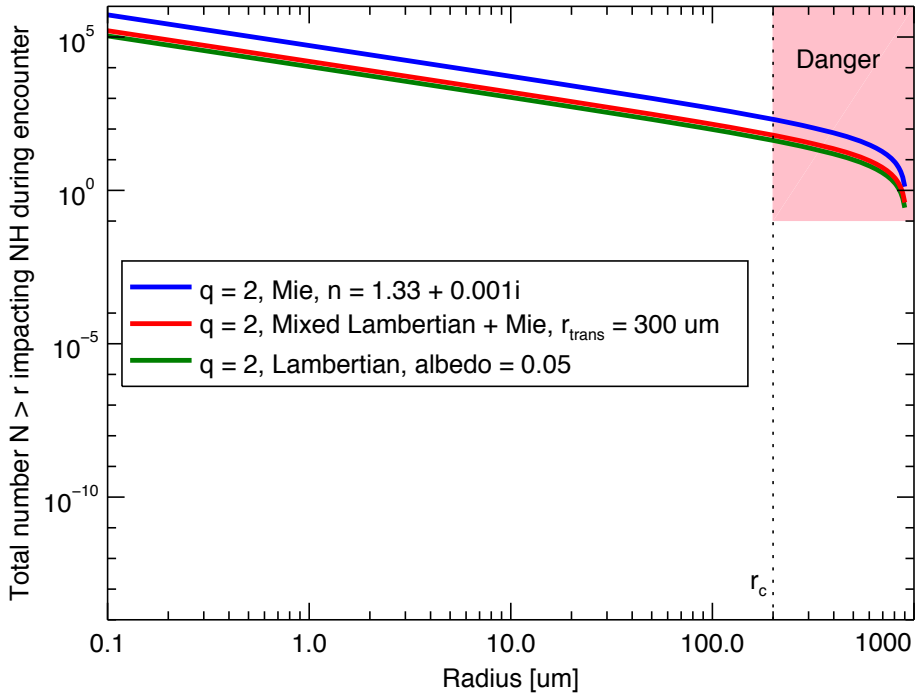

Fig. 7.— Dust population implied for rings made of a superposition of Mie and Lambertian scatterers. The middle curve is a combination of these two scattering models. In the case of $q = 2$, the ring is dominated by large grains and so the Mixed phase curve lies close to the Lambertian one. For $q > 3$, the dominance of small grains causes the Mixed curve to lie closer to the Mie phase curve. Any plausible scatterer should lie between the two end-member cases.

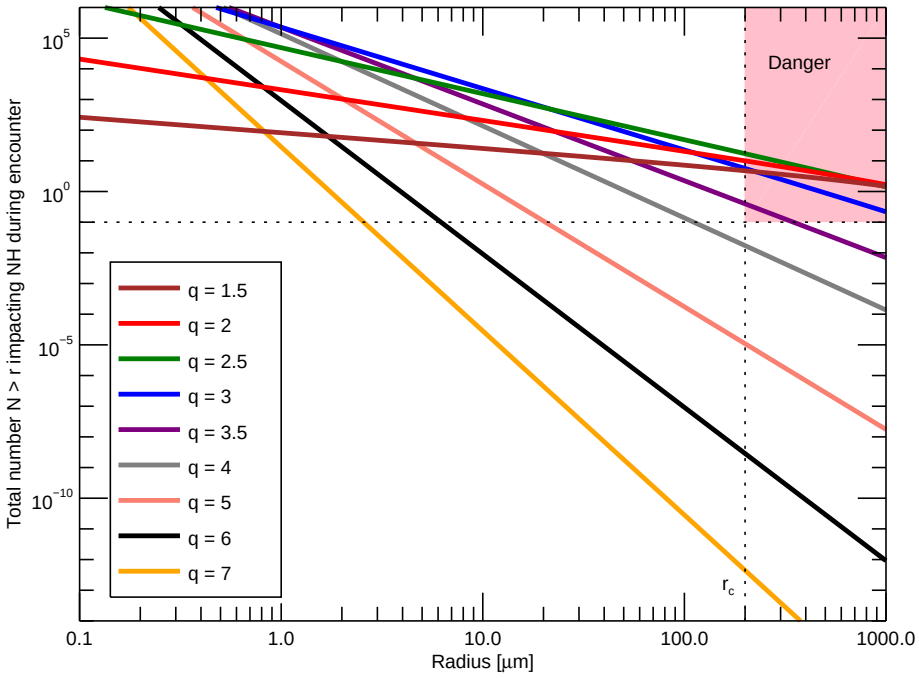

Fig. 8.— Constraints on dust population from HST observations. The lines indicate the different populations of grains with different size distributions. The visible I/F of all of the lines is identical and matches the 2012 HST-derived upper limit. The red quadrant indicates a population of particles that exceed the NH mission requirement of $N(r > r_c) < 0.1$. Our results place a limit of $N \lesssim 20$ particles of size r_c (green curve).

their unpublished data.

REFERENCES

Assafin, M., J. Camargo, R. V. Martins, A. H. Andrei, B. Sicardy, L. Young, D. N. da Silva Neto, and F. Braga-Ribas, 2010, Precise predictions of stellar occultations by Pluto, Charon, Nix, and Hydra for 2008–2015. *Astron. & Astrophys.* **515**.

Boissel, Y., B. Sicardy, F. Roques, P. Gaulme, A. Doressoundiram, T. Widemann, S. P. Littlefair, T. R. Marsh, M. Assafin, F. Braga-Ribas, V. Ivanov, D. da Silva Neto, O. Marco, E. Mason, J. I. B. Camargo, A. Andrei, N. Ageorges, O. Mousis, R. Vieira Martins, R. Behrend, P. Rousselot, M. Kretlow, and V. S. Dhillon, 2014, An exploration of Pluto's environment through stellar occultations. *Astron. & Astrophys.* **561**(A144), 1–11.

Braga-Ribas, F., B. Sicardy, J. L. Ortiz, C. Snodgrass, F. Roques, R. Vieira-Martins, J. I. B. Camargo, M. Assafin, R. Duffard, E. Jehin, J. Pollock, R. Leiva, M. Emilio, D. I. Machado, C. Colazo, E. Lellouch, J. Skottfelt, M. Gillon, N. Ligier, L. Maquet, G. Benedetti-Rossi, A. R. Gomes, P. Kervella, H. Monteiro, R. Sfair, M. E. Moutamid, G. Tancredi, J. Spagnotto, A. Maury, N. Morales, R. Gil-Hutton, S. Roland, A. Ceretta, S. h. Gu, X. b. Wang, K. Harpsøe, M. Rabus, J. Manfroid, C. Opitom, L. Vanzi, L. Mehret, L. Lorenzini, E. M. Schneiter, R. Melia, J. Lecacheux, F. Colas, F. Vachier, T. Widemann, L. Almenares, R. G. Sandness, F. Char, V. Perez, P. Lemos, N. Martinez, U. G. Jørgensen, M. Dominik, F. Roig, D. E. Reichart, A. P. LaCluyze, J. B. Haislip, K. M. Ivarsen, J. P. Moore, N. R. Frank, and D. G. Lambas, 2014, A ring system detected around the Centaur (10199) Chariklo. *Nature* **508**(7494), 72–75.

Buie, M. W., 1996, CCDPHOT—An IDL Widget Based CCD Photometry Reduction System. In *Astronomical Data Analysis Software and Systems V* (eds. G. H. Jacoby and J. Barnes), ASP Conferences Series 101.

Colwell, J. E., L. W. Esposito, R. G. Jerousek, M. Sremcevic, D. Pettis, and E. T. Bradley, 2010, Cassini UVIS stellar occultation observations of Saturn's rings. *Astron. J.* **140**, 1569–1578.

Cuzzi, J. N., 1985, Rings of Uranus: Not so thick, not so black. *Icarus* **63**, 312–316.

Durda, D. and S. A. Stern, 2000, Collision Rates in the Present-Day Kuiper Belt and Centaur Regions: Applications to Surface Activation and Modification on Comets, Kuiper Belt Objects, Centaurs, and Pluto–Charon. *Icarus* **145**(1), 220–229.

Durda, D. D., G. J. Flynn, L. E. Sandel, and M. M. Strait, 2007, Size-frequency distributions of dust-size debris from the impact disruption of chondritic meteorites. In *Dust in Planetary Systems Conference*.

Elliot, J. L., E. Dunham, and D. Mink, 1977, The rings of Uranus. *Nature* **267**, 328–330.

Elliot, J. L., M. J. Person, A. Gulbis, S. P. Souza, E. R. Adams, B. A. Babcock, J. W. Gangestad, A. E. Jaskot, E. A. Kramer, and J. M. Pasachoff, 2007, Changes in Pluto's atmosphere: 1988-2006. *Astron. J.* **134**(1), 1.

Giuliatti Winter, S. M., O. C. Winter, E. Vieira Neto, and R. Sfair, 2013, Stable regions around Pluto. *Mon. Not. Royal Astro. Soc.* **430**(3), 1892–1900.

Guinan, E. F., C. C. Harris, and F. P. Maloney, 1982, Evidence for a ring system of Neptune. *BAAS* **14**, 658.

McDonald, S. W. and J. L. Elliot, 2000, Pluto-Charon Stellar Occultation Candidates: 2000-2009. *Astron. J.* **119**(4), 1999–2007.

McKay, A., 2008, *Using Occultations to Study the Pluto-Charon System, Asteroids, and Cometary Comae*. Undergraduate thesis, Williams College.

Pasachoff, J. M., B. A. Babcock, S. P. Souza, J. W. Gangestad, A. Jaskot, J. L. Elliot, A. A. Gulbis, M. J. Person, E. A. Kramer, E. R. Adams, C. A. Zuluaga, R. E. Pike, P. J. Francis, R. Lucas, A. S. Bosh, D. J. Ramm, J. G. Greenhill, A. B. Giles, and S. W. Dieters, 2006, A search for rings, moons, or debris in the Pluto system during the 2006 July 12 occultation. *DPS* **38**, 2502.

Pires dos Santos, P. M., S. M. Giuliatti Winter, R. Sfair, and D. C. Mourao, 2013, Small particles in Pluto's environment: effects of the solar radiation pressure. *Mon. Not. Royal Astro. Soc.* **430**(4), 2761–2767.

Showalter, M. R., H. A. Weaver, A. Stern, A. J. Steffl, D. P. Hamilton, M. W. Buie, W. J. Merline, L. A. Young, M. Mutchler, R. Soummer, and H. B. Throop, 2012, Pluto's P4 and P5: Latest Results for Pluto's Tiniest Moons. *DPS* **44**.

Steffl, A. J. and S. A. Stern, 2007, First constraints on rings in the Pluto system. *Astron. J.* **133**, L1485–1489.

Stern, S. A., H. A. Weaver, A. J. Steffl, M. J. Mutchler, W. J. Merline, M. W. Buie, E. F. Young, L. A. Young, and J. R. Spencer, 2006, A giant impact origin for Pluto's small moons and satellite multiplicity in the Kuiper belt. *Nature* **439**, 946–948.

Throop, H. B. and L. W. Esposito, 1998, G ring particle sizes derived from ring plane crossing observations. *Icarus* **131**, 152–166.

Throop, H. B., S. A. Stern, J. W. Parker, G. R. Gladstone, and H. A. Weaver, 2009, Introducing GV : The Spacecraft Geometry Visualizer. *DPS* **41**.

van Belle, G. T., 1999, Predicting Stellar Angular Sizes. *Pub. Astro. Soc. Pac.* **111**(7), 1515–1523.

Young, E. F., R. G. French, L. A. Young, C. R. Ruhland, M. W. Buie, C. B. Olkin, J. Regester, K. Shoemaker, G. Blow, J. Broughton, G. Christie, D. Gault, B. Lade, and T. Natusch, 2008, Vertical structure in Pluto's atmosphere from the 2006 June 12 stellar occultation. *Astron. J.* **136**, 1757–1769.

Young, E. F., L. A. Young, C. B. Olkin, M. W. Buie, K. Shoemaker, R. G. French, and J. Regester, 2011, Development and Performance of the PHOT (Portable High-Speed Occultation Telescope) Systems. *Pub. Astro. Soc. Pac* **123**, 735–745.